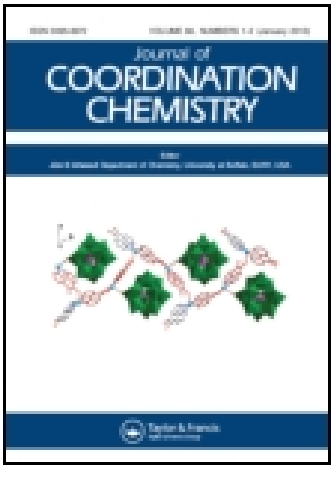

Journal of Coordination Chemistry
Publication details, including instructions for authors and subscription information:
http://www.tandfonline.com/loi/gcoo20

Synthesis, crystal structures, in vitro anticancer, and in vivo acute oral toxicity studies of bis-imidazolium/benzimidazolium salts and respective dinuclear Ag(I)-N-heterocyclic carbene complexes

Rosenani A. Haque[a], Noorhafizah Hasanudin[a], Muhammad Adnan Iqbal[a], Ashfaq Ahmad[c], Suzana Hashim[b], Ams Abdul Majid[b] & Mohamed B. Khadeer Ahamed[b]

[a] The School of Chemical Sciences, Universiti Sains Malaysia, Minden, Malaysia

[b] EMAN Testing and Research Laboratory, The School of Pharmaceutical Sciences, Universiti Sains Malaysia, Minden, Malaysia

[c] The School of Pharmaceutical Sciences, Universiti Sains Malaysia, Minden, Malaysia

Accepted author version posted online: 02 Aug 2013.Published online: 02 Sep 2013.

To cite this article: Rosenani A. Haque, Noorhafizah Hasanudin, Muhammad Adnan Iqbal, Ashfaq Ahmad, Suzana Hashim, Ams Abdul Majid & Mohamed B. Khadeer Ahamed (2013) Synthesis, crystal structures, in vitro anticancer, and in vivo acute oral toxicity studies of bis-imidazolium/benzimidazolium salts and respective dinuclear Ag(I)-N-heterocyclic carbene complexes, Journal of Coordination Chemistry, 66:18, 3211-3228, DOI: 10.1080/00958972.2013.831406

To link to this article: http://dx.doi.org/10.1080/00958972.2013.831406

Journal of Coordination Chemistry, 2013
Vol. 66, No. 18, 3211–3228, http://dx.doi.org/10.1080/00958972.2013.831406

Synthesis, crystal structures, *in vitro* anticancer, and *in vivo* acute oral toxicity studies of bis-imidazolium/benzimidazolium salts and respective dinuclear Ag(I)-*N*-heterocyclic carbene complexes

ROSENANI A. HAQUE*†, NOORHAFIZAH HASANUDIN†, MUHAMMAD ADNAN IQBAL*†, ASHFAQ AHMAD§, SUZANA HASHIM‡, AMS ABDUL MAJID‡ and MOHAMED B. KHADEER AHAMED‡

†The School of Chemical Sciences, Universiti Sains Malaysia, Minden, Malaysia
‡EMAN Testing and Research Laboratory, The School of Pharmaceutical Sciences, Universiti Sains Malaysia, Minden, Malaysia
§The School of Pharmaceutical Sciences, Universiti Sains Malaysia, Minden, Malaysia

(*Received 3 May 2013; accepted 19 July 2013*)

The synthesis, spectral (FT-IR and NMR), and structural studies of 1,1′-methylene linked 3,3′-2-cyanobenzyl bis-imidazolium salt ($\mathbf{L}_1$) and respective dinuclear Ag(I)-NHC complex ($\mathbf{C}_1$) are reported. The structures of both compounds were established through single-crystal X-ray diffraction. $\mathbf{C}_1$ has a short Ag–Ag separation of 3.16 Å. Both $\mathbf{L}_1$ and $\mathbf{C}_1$ were tested for potential against leukemia (k562) cell line. For comparison, *para*-xylyl linked bis-benzimidazolium salts ($\mathbf{L}_2$–$\mathbf{L}_4$) and their dinuclear Ag(I)-NHC complexes ($\mathbf{C}_2$–$\mathbf{C}_4$) were synthesized and tested against the same cell line (K562). The IC_{50} values proved that $\mathbf{L}_2$–$\mathbf{L}_4$ and $\mathbf{C}_2$–$\mathbf{C}_4$ are many fold more active than $\mathbf{L}_1$ and $\mathbf{C}_1$. The mechanism of action and structure activity relationship are discussed. *In vivo* oral acute toxicity study (sighting study) was carried out which depicts that 2000 mg/kg dose of selected compounds is an appropriate and safe dose for conducting main study on animals.

Keywords: Ag(I)-*N*-heterocyclic carbene; Anticancer; K562; Crystal structure; Ag–Ag separation; SAR; Acute oral toxicity

Introduction

N-heterocyclic carbenes (NHCs) are readily accessible in a few steps from azolium (imidazolium, benzimidazolium, etc.) salts which are stable compounds [1]. In these carbenes, a divalent carbon is flanked by two π-donor nitrogens. The strong σ-donating and weak π-accepting properties of NHCs make them excellent ligands for d-block [2] and f-block elements [3, 4]. NHCs have been bonded to almost all transition metals using different synthetic routes, and the complexes have been tested for catalytic and biomedical applications [2, 4–10]. Among various metal NHC complexes, Ag(I)-NHC complexes have been synthesized most widely [11].

*Corresponding authors. Email: rosenani@usm.my (R.A. Haque); adnan_chem38@yahoo.com (M.A. Iqbal)

Since the first synthesis of a Ag(I)-*N*-heterocyclic carbene complex in 1993 [12], this class of compounds has been extensively used for transmetallation reactions where direct synthesis using other metal ions was difficult or impossible [9]. These complexes are valuable due to their ease of synthesis, ease of handling, and air and moisture stability. Ag (I)-NHC complexes were tested for catalytic potential [13–15] but were less effective compared to other organometallic compounds [6, 16–19]. However, these compounds have vital antimicrobial activity [20–24]. In 2007, Youngs *et al.* [25] reviewed these compounds as a new class of antibiotics. These compounds were tested and corroborated by recent reports [26–28] and reviews [29–31]. Several mononuclear Ag(I)-NHC complexes with coordination motifs A-C (chart 1) have been studied [20, 27, 32–35]. Dinuclear Ag(I)-NHC complexes of structure D have recently been introduced as potential anticancer agents [36–46].

Dinuclear Ag(I)-NHC complexes, derived from *para*-xylyl linked bis-benzimidazolium salts, exhibited anticancer activity against human colon cancer (HCT 116) and leukemia (HL-60) [36, 43, 47]. We reported synthesis, crystal structure, and anticancer potential of a dinuclear Ag(I)-NHC complex, where the dinuclear silver carbene complex was aggregated in pair with a short Ag–Ag separation [44]. In the present study, we present the structure of another imidazole-based dinuclear Ag(I)-NHC complex ($\mathbf{C}_1$), where the two neighboring silver ions within the same molecule have a close interaction of 3.16 Å. $\mathbf{L}_1$ and $\mathbf{C}_1$ were tested for their antiproliferative potential against chronic myelogenous leukemia (K562) cells. For comparison, other *para*-xylyl linked bis-benzimidazolium salts ($\mathbf{L}_2$–$\mathbf{L}_4$) and dinuclear silver (I)-NHC complexes ($\mathbf{C}_2$–$\mathbf{C}_4$) were synthesized and applied on the same cell line (K562).

According to the global cancer statistic report for all types of cancer, 10.9 million new cancer cases were registered in 2002 and 6.7 million patients died; whereas in 2008, this figure increased to 12.6 million new cancer cases and 7.5 million deaths [48]. From leukemia (blood cancer), every year 300,000 patients are registered and about 222,000 patients die [48]. The ratio of deaths/cases (74%) represents the fatality of this specific type of cancer. Rapid development in anticancer drug discovery is necessary and the current study is an effort to contribute.

Experimental

Reagents and instruments

Nuclear magnetic resonance spectra were recorded on a Bruker 500 MHz Ultrashield™ spectrometer at ambient temperature. ^{1}H and ^{13}C NMR peaks are labeled as singlet (s),

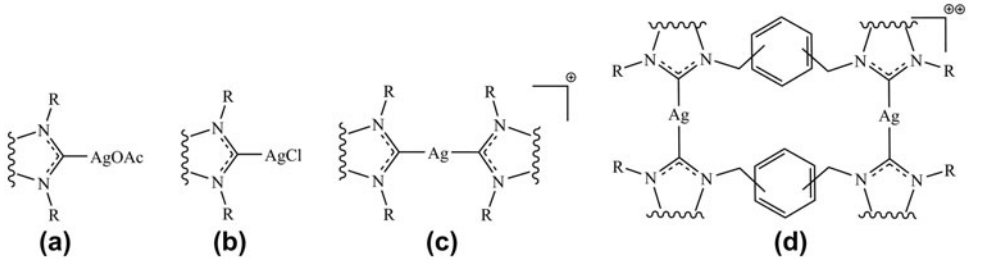

Chart 1. Silver(I)-N-heterocyclic carbene complexes with different coordination motifs studied for their anticancer potential. Structure D, the un-specified positions represent ortho/meta/para units. R is either alkyl or aryl substitution.

doublet (d), triplet (t), and multiplet (m). Chemical shifts were referenced with respect to solvent signals. FT-IR spectra were recorded on a Perkin–Elmer-2000. Elemental analysis was carried out on a Perkin–Elmer series II, 2400 microanalyzer. X-ray diffraction data were taken with a Bruker SMART APEX2 CCD area-detector diffractometer. The melting and boiling points were assessed by using a Stuart Scientific SMP-1 (UK) instrument. Chemicals and solvents were used as received.

RPMI 1640 media were purchased from ScienCell, USA. Heat inactivated fetal bovine serum (HIFBS) was obtained from GIBCO, UK. Phosphate-buffered saline (PBS), penicillin/streptomycin (PS) solution, MTS reagent and the reference standard, 5-fluorouracil were purchased from Sigma–Aldrich, Germany. All other chemicals used in this study were analytical grade.

Cell line and culture conditions

Human immortalized myelogenous leukemia cell line (K562) was purchased from American Type Culture Collection (Rockville, MD, USA). K562 cell line is the erythroleukemia type and is derived from a female chronic myelogenous leukemia patient in blast crisis. The cells were maintained in RPMI 1640 culture medium with 10% HIFBS and 1% PS. Cells were cultured in 5% CO_2-humidified atmosphere at 37 °C.

Synthesis

Synthesis of 1,1′-methylene bis(imidazole). To a stirring solution of imidazole (3.0 g, 44 mM) in 100 mL of dichloromethane, potassium hydroxide (4.94 g, 88 mM) was added. The mixture was refluxed at 50 °C for 12 h. The solvent was decanted and volatiles were removed to afford 1,1-methylene bis(imidazole) as a white solid, washed with ether and dried. General reaction involved in the preparation of the title compound is shown in scheme 1. White powder. Yield: 3.82 g (60%). ^{1}H NMR (500 MHz, DMSO-d_6): 6.21 (2H, s, 1 × CH_2), 6.91 (2H, s, 1 × CH, imidazole), 7.39 (2H, s, 1 × CH, imidazole), 7.9 (2H, s, 2 × NCHN); ^{13}C{^{1}H NMR} (125.1 MHz, DMSO-d_6): 54.8 (2 × CH_2, methylene), 119.0 (2 × CH, imidazole-C4), 129.1 (2 × CH, imidazole-C5), 137.5 (2 × NCN).

Synthesis of 1,1′-methylenebis{3-(2-cyanobenzyl)-imidazolium} dibromide (L_1). 2-(Bromomethylene)-benzonitrile (2.65 g, 13.6 mM) was added to a stirring solution of 1,1′-methylene bis(imidazole) (1.0 g, 6.8 mM) in 1,4-dioxane (100 mL). The mixture was refluxed at 100 °C for 24 h and the solution was evaporated under vacuum to yield a brownish thick fluid ($\mathbf{L}_1$). To purify, the bromide salt was directly converted to its hexafluorophosphate (PF_6^-) salt by metathesis using potassium hexafluorophosphate (KPF_6) (1.25 g, 6.8 mM) in 50 mL of methanol; the mixture was stirred for 3 h. The salt was obtained as a white crystalline solid. Single crystals suitable for X-ray diffraction were obtained by exposing a saturated solution of $\mathbf{L}_1.2PF_6$ in acetonitrile to the vapors of diethyl ether at room temperature. For characterization, the PF_6 salt of $\mathbf{L}_1$ was used whereas for further synthesis halide salt was used. Colorless cubes. Yield 1.8 g (49%), mp: 192–194 °C. ^{1}H NMR (500 MHz, DMSO-d_6): 5.74 (4H, s, 2 × N_{imid}–CH_2–Ar), 6.67 (4H, s, 2 × N_{imid}–CH_2–N_{imid}), 7.53 (2H, d, 2 × CH imidazolium H5′, J = 7.5 Hz), 7.63 (2H, t, Ar-H), 7.66 (2H, t, Ar–H), 7.82 (2H, m, Ar–H), 7.89 (2H, t, Ar–H), 7.99 (2H, d, 2 × CH imidazolium H4′, J = 7.5 Hz), 8.05

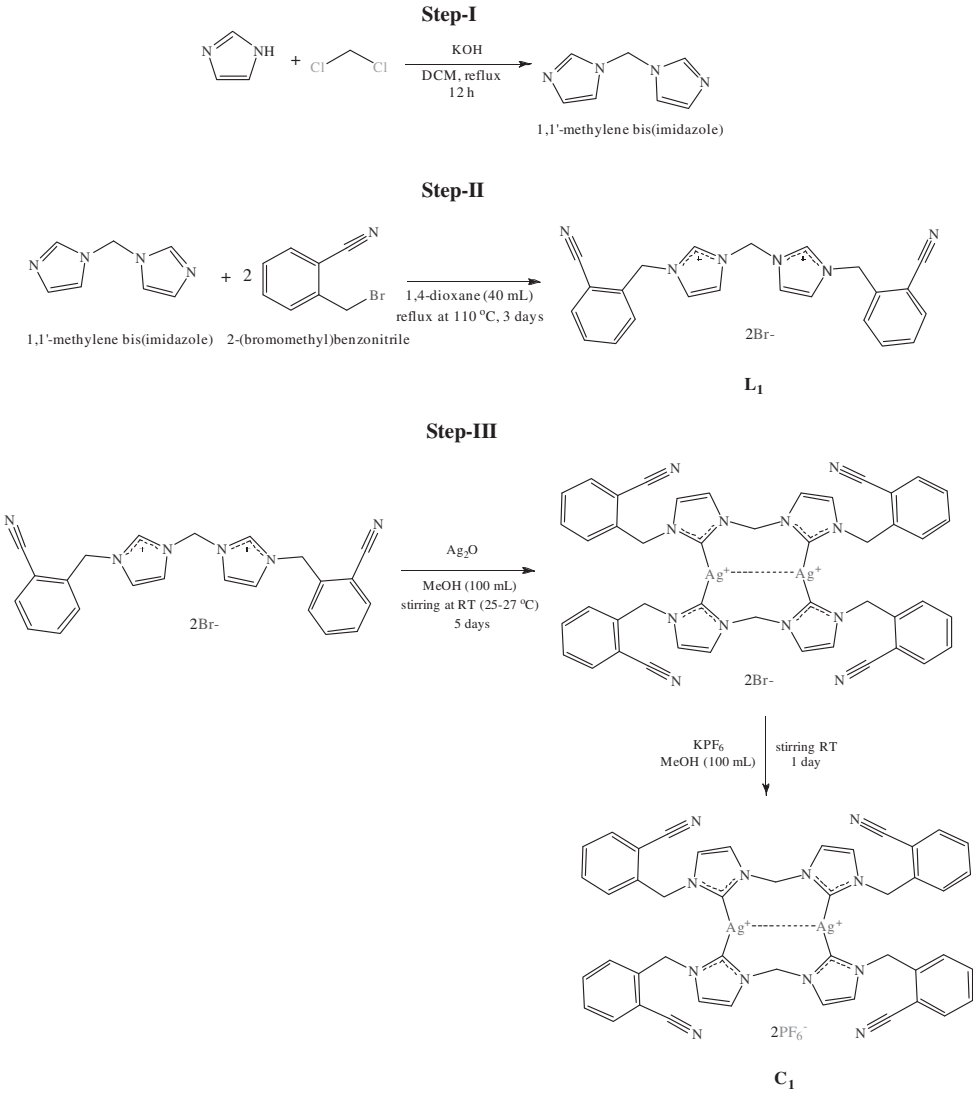

Scheme 1. Synthesis of 1,1′-methylene bis(imidazole), 1,1′-methylenebis{3-(2-cyanobenzyl)-imidazolium}dibromide ($\mathbf{L}_1$), and respective dinuclear Ag-NHC complex ($\mathbf{C}_1$).

(2H, s, Ar–H), 9.52 (2H, s, 2 × NCHN); $^{13}C\{^1H$ NMR} (125.1 MHz, DMSO-d_6): 50.7 (2 × N_{imid}–C–Ar, methylene), 58.5 (2 × N_{imid}–C–N_{imid}, methylene), 122.8, 129.6 (imidazolium C5′ and C4′), 111.1 (CN), 116.7, 133.7, 134.0, 136.8 (Ar–C), 138.4 (NCN). FT-IR (KBr): υ (cm^{-1}); 3422 (C_{aliph}–N_{imid}); 3159, 3104, 3061 (C–H_{arom}); 2972 (C–H_{aliph}); 2227 (C=N) 1604, 1578, 1555 (C_{arom}–C_{arom}); 1446, 1410, 1361, 1335 (C_{imid}–N_{imid}). Anal. Calcd for $\mathbf{C}_{23}H_{22}F_{12}N_6O_1P_2$: C, 41.21; H, 3.01; N, 12.54%. Found: C, 41.18; H, 3.04; N, 12.40%.

3,3′-(1,4-Phenylenebis(methylene))*bis*(1-alkyl-benzimidazolium) salts (L_2–L_4). Synthesis and characterization of *para*-xylyl linked bis-benzimidazolium salts (L_2–L_4) were carried out according to the literature procedure (scheme S1) [39].

Synthesis of imidazole-based dinuclear Ag(I)-NHC complex (C_1). L_1.2Br (1.5 g, 4 mM) was dissolved in methanol (100 mL) along with Ag_2O (0.64 g, 3 mM) with exclusion of light by covering the flask with aluminum foil. The reaction mixture was stirred for 5 days at room temperature. The reaction mixture was filtered by Celite 545 to collect a clear solution, converted directly to its hexafluorophosphate counterpart by metathesis reaction using KPF_6 (0.56 g, 3 mM) in 40 mL of methanol/water mixture (1 : 1). The white precipitate was collected and washed with fresh methanol (2 × 3 mL) to give the product as a white powder that was further recrystallized by acetonitrile/water. Single crystals suitable for X-ray diffraction were obtained by exposing a saturated solution of C_1.2PF_6 in acetonitrile to the vapors of diethyl ether at room temperature. Colorless cubes. Yield 2.7 g (58%), mp: 198–200 °C. ^{1}H NMR (500 MHz, DMSO-d_6): 5.44 (8H, s, 4 × N_{imid}–CH_2–Ar), 6.67 (8H, s, 4 × N_{imid}–CH_2–N_{imid}), 7.15 (2H, d, 2 × CH imidazolium H5′, J = 8.0 Hz), 7.45 (2H, t, Ar–H), 7.52 (2H, s, Ar–H), 7.62 (2H, m, Ar–H), 7.75 (2H, d, 2 × CH imidazolium H4′, J = 7.5 Hz), 7.90 (2H, s, Ar–H), 7.90 (2H, s, Ar-H); ^{13}C{^{1}H NMR} (125.1 MHz, DMSO-d_6): 52.7 (4 × N_{imid}–C–Ar, methylene), 63.6 (4 × N_{imid}–C–N_{imid}, methylene), 122.5, 128.9 (imidazolium C5′ and C4′), 110.1 (CN), 116.9, 133.4, 134.4, 139.2 (Ar-C) and 181.6 & 183.1 [d, $^1J_{(Ag109\text{-}Ccarbene)}$ = 183.75 Hz & d, $^1J_{(Ag107\text{-}Ccarbene)}$ = 208.78 Hz]. FT-IR (KBr): υ (cm^{-1}); 3422 (C_{aliph}–N_{imid}); 3176, 3140, 3117 (C–H_{arom}); 2979 (C–H_{aliph}); 2231 (C=N); 1601, 1578 (C_{arom}–C_{arom}); 1453, 1423, 1401, 1374, 1351, 1335 (C_{imid}–N_{imid}). Anal. Calcd for $C_{46}H_{36}Ag_2F_{12}N_{12}P_2$: C, 43.762; H, 3.18; N, 13.28%. Found: C, 43.62; H, 3.00; N, 13.30%.

Synthesis of benzimidazole-based dinuclear Ag(I)-NHC complexes (C_2–C_4). Synthesis and characterization of benzimidazole-based silver(I) *N*-heterocyclic carbene complexes (C_2–C_4) were carried out according to the literature procedure (scheme S1) [39].

Preparation of cell culture

Initially, K562 cell line was allowed to grow under optimal incubator conditions. Cells that reached a confluence of 70–80% were chosen for cell plating purposes. Old medium was replaced centrifugally with fresh medium after washing the cells using sterile PBS (pH 7.4) 2–3 times. Cells were incubated at 37 °C in 5% CO_2 for 1 min. Then, the flasks containing the cells were observed under inverted microscope (to confirm adequate proliferation of cells). Cells were counted and diluted to get a final concentration of 2.5 × 10^5 cells/mL and inoculated into wells (100 µL cells/well). Finally, plates containing the cells were incubated at 37 °C with an internal atmosphere of 5% CO_2.

MTS assay

Cancer cells (100 µL cells/well, 1.5 × 10^5 cells/mL) were inoculated in a 96-well microtiter plate. Then, the plate was incubated overnight in a CO_2 incubator to allow for acclimatization. Various concentrations of 100 µL of test substance were added into each well containing

the cells. Test substance was diluted with media into the desired concentrations from the stock. The plates were incubated at 37 °C with an internal atmosphere of 5% CO_2. After 48 h treatment period, 50 µL of MTS reagent (2 mg/mL) was added into each well and incubated again for 4 h. Following the incubation period, the medium containing MTS was aspirated from each well, and 100 µL of DMSO was added to dissolve formazan and read the absorbance of soluble formazan. The absorbance of soluble formazan was read at 570 and 620 nm wavelengths using a high-end Tecan M200Pro multimode microplate reader. Data were recorded and analyzed for the assessment of the effects of test substance on cell viability and growth inhibition. The percentage of growth inhibition was calculated from the optical density obtained from MTS assay. 5-FU was used as the standard reference drug.

In vivo *acute oral toxicity tests*

Selection, preparation and grouping of animals. Rodents like rats are used for acute oral toxicity dose methods with females more sensitive than males. Female rats were obtained from Animals Research and Service Center (ARASC) USM Main campus under approval of Grant No. USM/Animals Ethics Approval/2012/(76) (364). Female rats were selected randomly, marked for identification, and kept in cages for at least 5 days in an animal transient room. Animals were acclimatized to laboratory conditions prior to the start of dosing for acute oral toxicity sighting study. All the animals were nulliparous and non-pregnant, and their weight was 210 g ± 10. The rats were divided into five groups. Two were marked with (benz)imidazolium salts $\mathbf{L}_1$ and $\mathbf{L}_2$ and next two with $\mathbf{C}_1$ and $\mathbf{C}_2$, respectively. Finally, the last group was treated for vehicle containing water and minute quantity of Tween 80.

Preparation of doses. Solubility of these substances was enhanced by using Tween-80 in limited doses to avoid toxicity originating from it. However, care was exercised to avoid final volume not more than 1 mL/100 g of the body weight of animals as mentioned in OECD guidelines 420. Doses were prepared shortly before use as their stability of preparation should be known.

Acute oral toxicity tests. Purpose of this sighting study was to select the safe and appropriate dose for main study. An oral gavage tube was used to insert the single dose of selected compounds. Animals were fasted for 3–4 h before dose but water supply was not withheld. Test compounds were given to single dose in sequential manner following the flow chart in figure shown below as per OECD guidelines. The starting dose for the sighting study is selected from the fixed dose levels of 5, 50, 300, and 2000 mg/kg and considered as a dose expected to produce some evident toxicity based, when possible, on data obtained from *in vivo* and *in vitro* studies of structurally related compounds. A period of at least 24 h will be allowed between the dosing of each animal and they were observed for 14 days.

Results and discussion

Synthesis

Synthesis of $\mathbf{C}_1$ was carried out in three steps shown in scheme 1. In step-I, imidazole was converted to its potassium salt by refluxing two equivalents of potassium hydroxide with

one equivalent of imidazole. The potassium salt of imidazole was collected as white powder after decanting the reaction medium (1,4-dioxane) and directly reacted with dichloromethane under reflux. Solvent was evaporated; residue was washed with diethyl ether and dried at ambient temperature. In step-II, two equivalents of 2-(bromomethyl)-benzene were allowed to react with one equivalent of product obtained in step-I. The mixture was refluxed for 3 days in 1,4-dioxane. The use of 1,4-dioxane as a reaction medium for the synthesis of bis-(benz)imidazolium salts has advantages over other solvents (acetonitrile, dimethyl sulfoxide, etc.) due to its moderate polarity and low boiling point. Using 1,4-dioxane as a reaction medium, the bis-azolium salts can be either obtained as thick fluids at the bottom of the flask or powders. The desired compound was obtained either by decanting the reaction medium (thick fluid) or by filtering (white powder) [39, 43, 44]. Similarly, in the current synthesis, $\mathbf{L}_1$ appeared as a thick yellowish fluid that was further converted to its PF_6 salt by metathesis in methanol to get it a white powder. Metathesis is usually performed to achieve further purity of such compounds as well as for the ease of handling. However, for the synthesis of respective dinuclear silver complexes, we prefer halide salts of these ligands. Hence, in step-III, one equivalent of halide salt of $\mathbf{L}_1$.2Br was dissolved in 100 mL of methanol along with silver oxide (1 equivalent) and the mixture was stirred for 5 days at room temperature with exclusion of light. Celite 545 was used to filter the mixture; filtration is usually repeated to get a crystal clear solution which is converted to its hexafluorophosphate salt (scheme 1).

Synthesis and characterization of $\mathbf{L}_2$–$\mathbf{L}_4$ and $\mathbf{C}_2$–$\mathbf{C}_4$ were carried out according to the reported procedure with minor modifications (scheme S1) [36].

FT-IR spectra of the compounds

Dinuclear Ag(I)-NHC complexes show some peaks comparable to ligands [39, 40, 43, 44]. For $\mathbf{L}_1$, strong to weak but sharp vibrations (3005–3449 cm^{-1}) indicate aromatic C_{sp2}–H stretches. The pure C_{sp3}–H stretch for $\mathbf{L}_1$ appeared at 2972 cm^{-1} ($C–H_{aliph}$), weak because of very few methylene hydrogens. A strong and sharp vibration is at 2227 cm^{-1} for nitrile (C≡N) stretch (Supplementary material; figure S1). Weak to strong peaks at 1555–1604 cm^{-1} represent the symmetric aromatic ring stretches (C=C). The stretch at 1200–1500 cm^{-1} specific for −HC=N− [39, 43] indicates *N*-heterocyclic carbene carbon bonding with silver and a characteristic “four fingers (f.fs)” pattern appears for dinuclear silver NHC complexes [39, 43]. Previously, for a number of benzimidazole-based dinuclear silver NHC complexes, such “four fingers (f.fs)” pattern was reported [39, 40, 43, 44]. For $\mathbf{C}_1$, such patterns were not observed; however, some changes compared to $\mathbf{L}_1$ were observed. For example, in $\mathbf{L}_1$, four peaks at 1335, 1361, 1410, and 1446 cm^{-1} changed to six peaks, 1335, 1351, 1374, 1410, 1423, and 1453 cm^{-1} (C_{imid}–N_{imid}). Also, some changes can be observed from 1555–1604 cm^{-1} as well as 3061–3159 cm^{-1} (figure S1). These ranges are for C=C and C–H stretches of aromatic systems and typical for such complexes [39, 43].

FT-NMR spectra of the compounds

FT-NMR characteristics of $\mathbf{L}_1$ and $\mathbf{C}_1$ were analyzed in DMSO-d_6 from 0 to 12 ppm for ^{1}H NMR and 0–200 ppm for ^{13}C NMR studies. ^{1}H NMR spectrum of $\mathbf{L}_1$ has a sharp singlet at 9.51 δ ppm ascribed to the imidazolium ring (NCHN) acidic proton, in accord with previous reports [38, 43, 49]. Peaks for benzylic ($Ar–CH_2–N_{imid}$) and methylene

(N_{imid}–CH_2–N_{imid}) protons appear at 5.74 and 6.67 δ ppm, respectively (figure S2). Synthesis of $\mathbf{C}_1$ was confirmed by disappearance of acidic (NCHN) proton and changes in benzylic signals [50]. Methylene (N_{imid}–CH_2–N_{imid}) signals in $\mathbf{C}_1$ were suppressed (figure S2), probably because NMR radiations (RF radiations) cannot interact properly with protons close to the metal ions and hence sharp signals are not generated.

$\mathbf{L}_1$ and $\mathbf{C}_1$ were further confirmed by ^{13}C NMR spectra. The spectrum of $\mathbf{L}_1$ displayed a peak at 138.4 δ ppm ascribed to the imidazole ring carbon (NCN). This signal for benzimidazole ligands is at 142–144 δ ppm [39, 43, 51]. Upon complexation with Ag, two doublets appear at *ca*. δ 182 for $\mathbf{C}_1$ with Ag–C coupling constants *ca.* 208 and 183 Hz (figure S3). These doublets appear in dimeric complexes of structure $[\mathbf{L}_2Ag_2]^{2+}$ due to carbene carbon bonding to C–Ag^{107} and C–Ag^{109}, respectively [39, 50, 52]. For benzimidazole-based Ag-NHC complexes, such doublets appear at *ca*. δ 189 with splitting patterns 180 Hz for Ag^{107} and 204 Hz for Ag^{109} [27, 53]. The signals for benzylic (Ar–C–N_{imid}) and methylene (N_{imid}–C–N_{imid}) carbons for $\mathbf{L}_1$ are at 50.7 and 58.6 ppm, respectively. These signals moved 2–4 ppm downfield in $\mathbf{C}_1$ (52.7 and 63.6 ppm), in accord with previous reports [38, 39, 43, 52, 54–56].

Crystallography

Single crystals of $\mathbf{L}_1$ and $\mathbf{C}_1$ suitable for X-ray diffraction were grown by exposing saturated solution of each in acetonitrile (0.5 mL) to diethyl ether at room temperature (vapor diffusion method). Single crystals appeared as colorless blocks. Crystal refinement data for $\mathbf{L}_1$ and $\mathbf{C}_1$ are provided in table 1; selected bond lengths and angles for $\mathbf{C}_1$ are tabulated in table 2. Distances and angles for $\mathbf{L}_1$ are provided in the supplementary data file (table S1). $\mathbf{C}_1$ crystallizes in the monoclinic space group with *P-21/c* (No. 14) symmetry whereas $\mathbf{L}_1$ grew in monoclinic space group with *P-1* (No. 2) symmetry. A perspective view of $\mathbf{L}_1$ and $\mathbf{C}_1$ has been shown in figure 1. Figure 1(a) shows that the ligand is comprised of a *bis*-imidazolium cation and two bromides with a water bonded through P–F - - H–O hydrogen bonding.

The presence of water in bis-imidazolium hexafluorophosphate salts is rarely observed whereas in similar bis-imidazolium/benz-imidazolium bromide salts it is very frequent [57–62]. This is consistent with their polarity compared to the salts with hexafluorophosphate as counter anions (less polar). Figure 1(a) shows that both imidazolium units are on either side of methylene, facing opposite directions at 110.0 (14)°. The internal ring angles at N2–C9–N3 and N4–$\mathbf{C}_1$5–N5 are 107.78 (15) and 108.55 (16), respectively. The crystal packing (figure S4) shows that the cationic and anionic components are connected through C–H–F hydrogen bonding in the 3-D network.

The Ag(I)-NHC complex (figure 1(b)) is comprised of two silver cations sandwiched by two $\mathbf{L}_1$ through NHC carbon and two hexafluorophosphates. Two neighboring silver ions have a close interaction of 3.16 Å. Similar interactions have been previously observed by us [44] and others [63] for various structures. The internal ring angles of imidazolium units N1–$\mathbf{C}_1$–N2 and N4–$\mathbf{C}_1$2–N5 are at 104.0 (2)° and 104.02 (19)°, respectively. These internal ring angles are 3–4° smaller than compared to the angles in $\mathbf{L}_1$ whereas angles at each nitrogen increase 2–3°. The NHC carbon, after bonding with Ag(I), shifts its charge density to the metal due to which the shape of imidazole ring deviates, as previously reported [39, 40]. Bond lengths between the Ag ion and carbene are Ag1–$\mathbf{C}_1$/$\mathbf{C}_1$2A = 2.101(2)/2.097(2) Å, in accord with those of other Ag-NHC complexes [26, 27, 43, 53, 56, 64].

Table 1. Crystal data and structure refinement details of $\mathbf{L}_1$ and $\mathbf{C}_1$.

	$\mathbf{L}_1$	$\mathbf{C}_1$
Formula	$C_{23}H_{20}N_6F_{12}P_2.H_2O$	$C_{46}H_{36}Ag_2N_{12}F_{12}P_2$
Formula weight	688.41	1262.55
Crystal system	Triclinic	Monoclinic
Space group	*P-1*(No. 2)	*P-21/c* (No. 14)
Unit cell dimensions		
a (Å)	8.4636(1)	12.1787(15)
b (Å)	11.6581(2)	16.182(2)
c (Å)	15.5520(2)	14.2623(14)
α (°)	69.641(1)	90
β (°)	84.252(1)	122.437(7)
γ (°)	70.027(1)	90
V (Å^3)	1351.82(4)	2372.2(5)
Z	2	2
Density (Calcd) (gm/cm^3)	1.691	1.768
Abs. Coeff. (mm^{-1})	0.276	0.990
F (000)	696	1256
Crystal size (mm)	0.17 × 0.24 × 0.39	0.20 × 0.26 × 0.27
Temperature (K)	100	100
Radiation (Å)	MoK_α 0.71073	MoK_α 0.71073
θ min, max (°)	2.0, 32.7	2.1, 32.5
Dataset	−12 : 12; −17 : 17; −23 : 22	−18 : 18; −24 : 24; −20 : 21
Tot.; Uniq. Data	31,413	56,227
$R_{(int)}$	0.027	0.051
Nref, Npar	9782, 452	8580, 334
R, wR_2, S	0.0548, 0.1636, 1.04	0.0358, 0.0970, 1.09

Table 2. Selected bond lengths (Å) and angles (°) of $\mathbf{C}_1$.

C4–C5	1.513(3)	C23–N4	1.450(3)	C14–C13	1.348(3)
C4–N2	1.462(3)	N4–C12	1.356(3)	C2–C3	1.346(4)
C1–N2	1.353(3)	C12–N5	1.355(3)	N4–C13	1.388(3)
C1–N1	1.356(4)	N5–C15	1.461(4)	N2–C3	1.387(3)
N1–C23	1.448(3)	C15–C16	1.471(3)	F1–P1	1.600(3)
Ag1–C1	2.101(2)				
Ag1–C12A	2.097(2)				
C5–C4–N2	111.41(19)		N5–C14–C13	106.8(2)	
C4–N2–C3	123.89(18)		C14–C13–N4	106.2(2)	
N2–C1–N1	104.0(2)		C13–N4–C23	124.22(19)	
N2–C4–C5	111.41(19)		N1–C2–C3	106.0(2)	
N1–C23–N4	111.16(17)		F1–P1–F2	179.12(13)	
N4–C12–N5	104.02(19)		F1–P1–F3	90.86(13)	
N5–C15–C16	114.2(2)				
C1–Ag1–C12A	165.71(8)				

Comparison of bond distances and angles between ligand and dinuclear complex is shown in figure 2. The two silver cations are connected to the carbene through $\mathbf{C}_1$–Ag1–$\mathbf{C}_1$2A and $\mathbf{C}_1$A–Ag1A–$\mathbf{C}_1$2 (165.78°) bridges. In previous reports, C_x–Ag–C_y angles were 171–178° [39, 40, 43, 44]. However, in the current study, a bent angle (165.78°) indicates that the Ag–Ag interaction influences the C_x–Ag–C_y linearity of bonding. The crystal packing (figure S5) shows that cationic and anionic components of $\mathbf{C}_1$ are connected via C–H–F hydrogen bonding in a 3-D network.

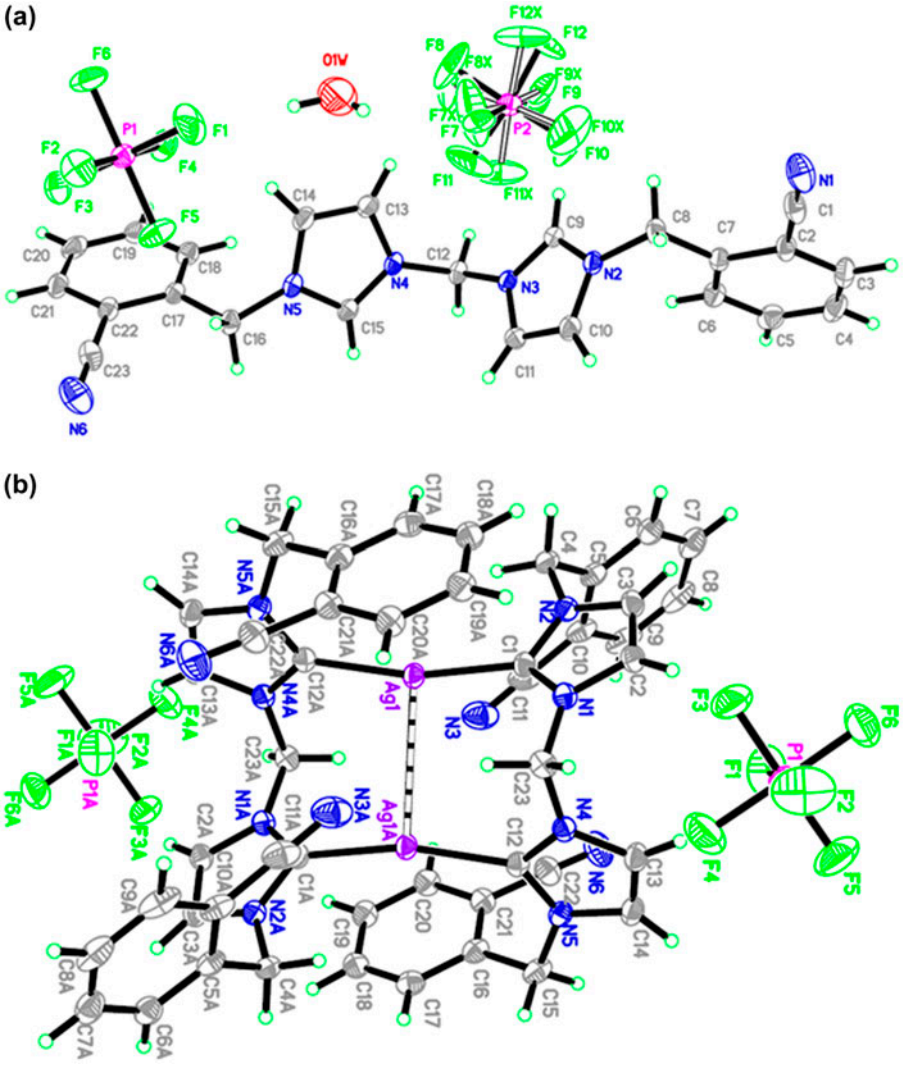

Figure 1. ORTEP of (a) *bis*-benzimidazolium salt $\mathbf{L}_1$ and (b) Ag(I)-NHC complex $\mathbf{C}_1$ with displacement ellipsoids drawn at 50% probability.

In vitro *anticancer activity*

Effect of $\mathbf{L}_1$ and $\mathbf{C}_1$ on proliferation of K562 cell line. A variety of heterocyclic compounds based on imidazole and benzimidazole are being studied as anticancer agents [29–31, 36, 65–71]. This is subject of recent reviews [29, 31, 70–72]. Thus, antiproliferative potencies of $\mathbf{L}_1$ and $\mathbf{C}_1$ were evaluated using MTS assay on cancer cell line, K562.

The antiproliferation test showed a dose-dependent effect of $\mathbf{C}_1$ on K562 cells whereas $\mathbf{L}_1$ proved to be inactive. Figure 3 illustrates the antiproliferative effect of test compounds. The graph clearly shows that $\mathbf{C}_1$ inhibited the proliferation of K562 cells in a dose-dependent manner parallel to 5-FU. In our previous reports, with benzimidazole, both the ligands

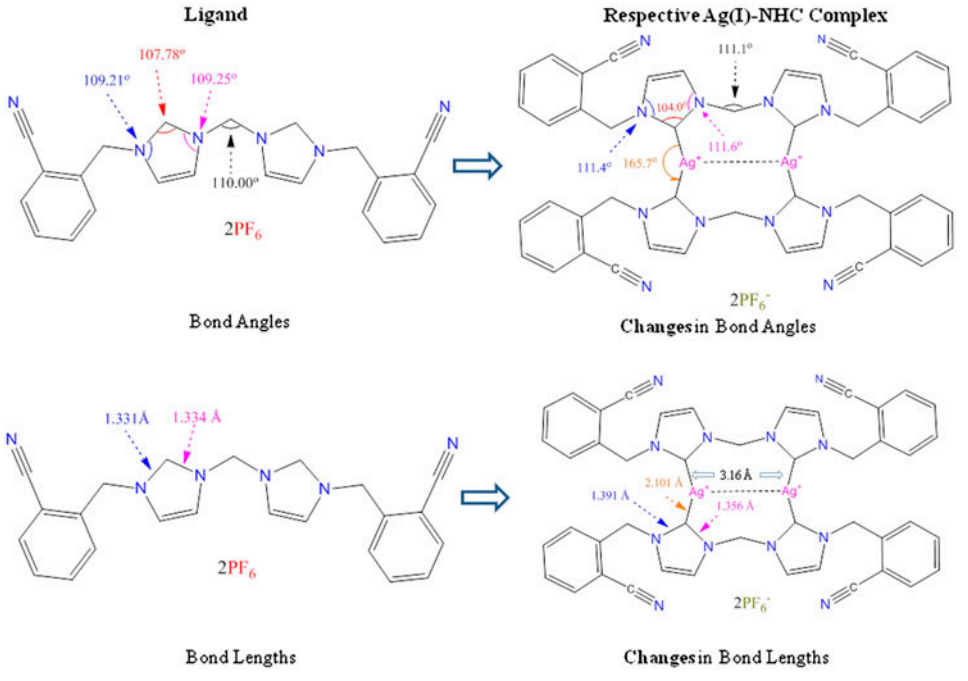

Figure 2. Comparison of selected bond angles and bond lengths between $\mathbf{L}_1$ and $\mathbf{C}_1$. All labeled values were selected from X-ray crystallographic data. The figure clearly shows that after bonding with Ag, the bond angle at carbene carbon (NCN) shrinks from 107.7° to 104.2° whereas the bond angles at both nitrogens expands 2–3°, that is, from 109.2° to 111.6°. This shows that the charge density drifted from imidazolium ring (ligand) to metal ion which causes deviation in ring shape. This phenomenon is further supported by significant changes in the C–N bond lengths as shown.

and xylyl linked dinuclear complexes showed anticancer activity against various cancer cell lines [43, 44, 49, 53], indicating relatively higher potential of benzimidazole compared to imidazole against cancer [68, 69]. However, the metal complexes of both of these moieties (imidazole and benzimidazole) show significant anticancer activity [21, 26, 27, 53, 73].

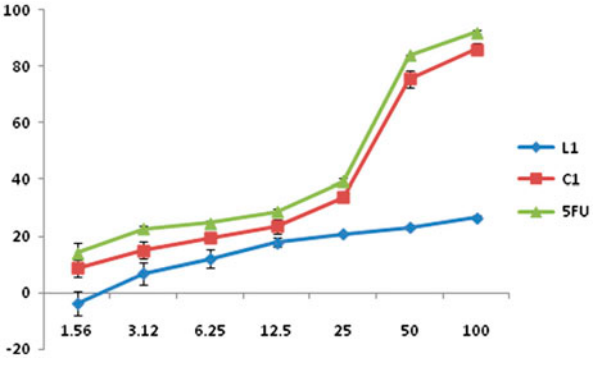

Figure 3. Dose-dependent antiproliferative effect of $\mathbf{L}_1$ and $\mathbf{C}_1$ on leukemia cells (K562).

Figure S6 shows the cell images of tested compounds and standard drug (5-FU) against K562 cells. Figure S6B clearly shows $\mathbf{L}_1$ has trivial effect (IC_{50} > 200 μM) on cancer cells whereas the silver complex had cytotoxicity (IC_{50} = 43.7 μM), see figure S6C. However, both the new compounds are comparable to or less potent than standard drug (IC_{50} = 35.9 μM, 5-FU).

Effect of bis-benzimidazolium salts ($\mathbf{L}_2$–$\mathbf{L}_4$) and respective silver complexes ($\mathbf{C}_2$–$\mathbf{C}_4$) on proliferation of K562 cell line. For comparison, benzimidazole-based bis-salts and dinuclear complexes were tested against the same cell line (K562). Figure S7 shows the cell images of $\mathbf{L}_2$–$\mathbf{L}_4$ and $\mathbf{C}_2$–$\mathbf{C}_4$ against leukemia (K562). This is evident from the graph (figure 4) and cell images (figure S7) that all the *p*-xylyl linked bis-benzimidazolium salts ($\mathbf{L}_2$–$\mathbf{L}_4$, IC_{50} = 8.9–34.9 μM) and silver complexes ($\mathbf{C}_2$–$\mathbf{C}_4$, IC_{50} = 3.37–6.50 μM) are many fold active than imidazole-based compounds, $\mathbf{L}_1$ (IC_{50}= > 200 μM) and $\mathbf{C}_1$ (IC_{50} = 43.7 μM) including standard drug (5-FU, IC_{50} = 35.9 μM), see table 3. These results support our previous reports [38–41, 43, 44, 52] on the significance of bezimidazole-based silver NHC complexes compared to imidazole-based ones [42].

Two reports [42, 52] containing synthesis and anticancer potential of *N*-^{i}Pr/-allyl substituted xylyl (ortho/meta/para) linked imidazolium/benzimidazolium salts and respective

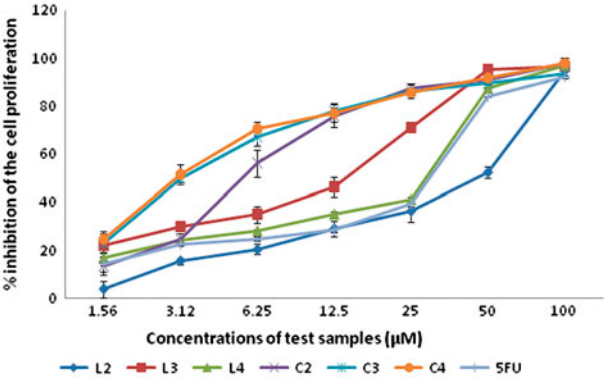

Figure 4. Dose-dependent antiproliferative effect of $\mathbf{L}_2$–$\mathbf{L}_4$ and $\mathbf{C}_1$–$\mathbf{C}_4$ on leukemia cells (K562).

Table 3. IC_{50} values of tested samples against K562 cell line.

Compound	*R*	Compounds	IC_{50} (μM) K562
Ligands	–	$\mathbf{L}_1$	>200
	octyl	$\mathbf{L}_2$	34.9
	nonyl	$\mathbf{L}_3$	8.9
	decyl	$\mathbf{L}_4$	9.0
Ag(I)–NHC complexes	–	$\mathbf{C}_1$	43.7
	octyl	$\mathbf{C}_2$	6.57
	nonyl	$\mathbf{C}_3$	3.67
	decyl	$\mathbf{C}_4$	3.37
Standard drug	–	5-FU	35.9

silver NHC complexes show that the *para*-xylyl linked complexes are active compared to complexes with *ortho* and *meta*. Bigger cavity size for these dinuclear complexes is better for the anticancer potential [42]. To further confirm this observation, $\mathbf{C}_1$ (scheme 1), with smaller cavity size, was compared with *para*-xylyl linked complexes ($\mathbf{C}_2$–$\mathbf{C}_4$, scheme S1), having bigger cavity size; $\mathbf{C}_2$–$\mathbf{C}_4$ were many fold more active than $\mathbf{C}_1$. These results support our argument of cavity size as mentioned above. This phenomenon can also be observed from a recent report [71] where imidazole-based *para*-xylyl linked dinuclear complexes showed much better antiproliferation activity compared to mononuclear silver NHC complexes against adenocarcinomas (MCF 7 and DLD1). The exact reasons of this behavior are not clear at this stage, however, but a detailed mechanistic study is in progress.

Mechanism of action and structure activity relationship

In the last decade, various silver(I) complexes have been studied for their antimicrobial potential [74–77]; these complexes release Ag^+ that bind with the bacterial cell surfaces and interact with the proteins involved in cell wall synthesis to disrupt the cell functions [78]. The scientific community believes that anticancer mechanism of silver(I) complexes is also monitored by release of silver ions and its binding with the proteins and DNA [79]. However, for antimicrobial potential of silver(I) complexes, the magnitude of activity was found to be related with the ease of the ligand displacement [79, 80]; for example, silver complexes with weak Ag–O or Ag–N bonds have a broader spectrum in their antimicrobial activities [81, 82]. In contrast, for anticancer potential of such silver(I) complexes, rapid release of Ag^+ lose their effect abruptly [30]. This drawback was compensated by introducing Ag-NHC complexes since *N*-heterocyclic carbenes (NHCs) are strong σ-donating and weak π-accepting ligands and release Ag^+ more slowly [30, 83–86].

Relatively higher anticancer potential of bis-benzimidazolium salts and dinuclear Ag(I)-NHC complexes in comparison with imidazole-based compounds might be due to association of benzene with the cellular system [86]. Researchers established a concept that benzene metabolites covalently interact with cellular macromolecules and produce toxicity [86–89]. Perhaps, this is the reason that bis-benzimidazolium salts and respective dinuclear complexes are relatively active compared to similar imidazole-based compounds [42]; however, this is a preliminary justification in favor of benzimidazole on the basis of literature. Further work is necessary to assess the actual reason of benzimidazole advantage over imidazole-based chemical moieties.

This research shows that human leukemia cells (K562) treated with silver complexes reveal characteristic features of apoptosis, evidenced through the membrane blebbing, chromatin condensation, and formation of apoptotic bodies (figures S6D and S7D, F, H). Our results support previous findings where silver(I)-NHC complexes induced caspase independent apoptotic cellular death via mitochondrial apoptosis-inducing factor [26]. Several studies have proved that silver cations deposit in the cytosol and render the cellular process defunct by interacting with rate-limiting enzymes and proteins that are crucial for essential biochemical pathways [25, 42, 90]. Thus, the present study reveals clear signs of black silver deposits in the cytoplasm of the affected cells (figures S6D and S7D, F, H), confirming that cytotoxic efficacy of the complexes is contributed by deposition of silver.

Increase in chain length increases the lipophilicity of complexes [36, 43] that probably further facilitates Ag(I)-NHC system to cross the cell wall barriers to interact with DNA and interrupt its function. Benzimidazole-based silver(I)-NHC complexes have already

shown strong DNA binding [37]. Table 3 clearly shows that with increase in chain length of *N*-alkyl substitution (octyl to decyl), the cytotoxicity of $\mathbf{L}_2$–$\mathbf{L}_4$ and $\mathbf{C}_2$–$\mathbf{C}_4$ increased.

Hence, the proper tuning of *N*-alkyl chain lengths, extension of benzene ring systems, and proper cavity size of such dinuclear Ag(I)-NHC complexes make them biologically valuable.

Preliminary in vivo *acute oral toxicity (sighting study)*

Acute toxicity is the observation of adverse effects occurring in an animal within a short time of administration of either a single dose of chemical or multiple doses given to the animal [91]. Acute toxicity test can provide better information about the biological properties of new chemical compounds than any other single test [92]. There are several methods to determine acute toxicity of a newly synthesized compound subject to the level of biological information required from it [91]. In the current study, "fixed-dose method" was adopted to determine the toxic dose by using sighting study [93]. The sighting study allows selection of the appropriate starting dose for the main *in vivo* study. In this method, the test substance is given orally among one of four fixed dose levels (5, 50, 300, and 2000 mg/kg) to animals. The purpose is to select a dose that produces signs of toxicity but no mortality [94]. The selection of starting dose depends upon the *in vivo* and *in vitro* data available in the literature for compounds having similar structure to the compound(s) undergoing the investigation; however, if such data are not available, 300 mg/kg is recommended as a starting dose for sighting study [93]. Depending on the results of the first test, either increased dose (2000 mg/kg) or lower doses (5 or 50 mg/kg) should be tested in case of mortality observed with 300 mg/kg dose. Figure 5 shows the chart for sighting study.

Initially, $\mathbf{L}_1$–$\mathbf{L}_2$ and $\mathbf{C}_1$–$\mathbf{C}_2$ were tested for sighting study using 300 mg/kg dose. Since the synthesized compounds were not soluble in saline, each compound (75 mg ± 5/210 g ± 10 of animal weight) was mixed with 300 µl of polysorbate 80 (Tween 80) in order to make the compound soluble and total volume was marked up to 2 mL with saline. To observe any possible toxicity due to polysorbate 80, 300 µL of it was separately dissolved in saline (1700 µL) and was orally given to a separate rat. No signs of toxicity due to polysorbate 80 were observed at given concentration.

All the animals after initial dose were observed after 20 min then after one hour and after that periodically at least once a day until the 14th day. Observation period was not made rigid as it depends upon the appearance of toxic reactions in animals. However subjected to the death of animal, the study should be certainly terminated immediately or if animal starts showing moribund symptoms, animal should be killed humanely. The body weight was also

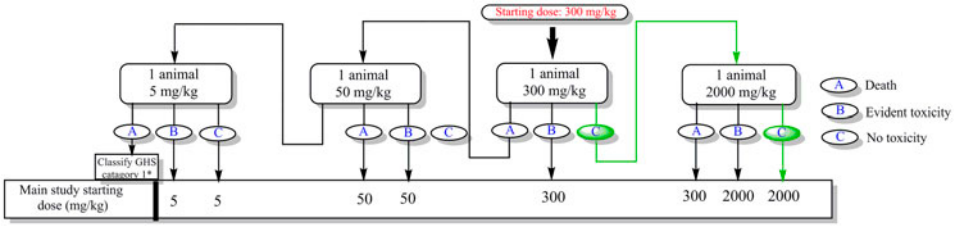

Figure 5. Sequential steps for sighting study. The green arrows indicate the path followed by the compounds.

observed. If weight reduction, moribund symptoms and diarrhea are observed during observational period then the dose should be labeled as toxic dose. However in the present study, all animals survived and remained healthy and agile. According to OECD guidelines, the quantity of test compounds was then increased to 2000 mg/kg of animal body weight and the same procedure of observation was repeated. No signs of toxicity were observed and animals remained alive, healthy, and agile. Hence, it is concluded that 2000 mg/kg body weight of these selected compounds can be the starting dose for main study. All the protocols of the study have been provided in the experimental section.

In vivo studies of Ag(I)-NHC complexes are rare. For example, 1 was tested on the ovarian cancer (OVCAR-3) using nude mice, whereas a high dose of 333 mg/kg caused a major cell death in the tumors without inducing any toxic effects to the major organs [35]. However, NHC complexes of Ru, Au, and Pt have been frequently studied using animals [29]. According to the best of our knowledge, this is the first time that dinuclear Ag(I)-NHC complexes were studied for their acute oral toxicity. The results will be beneficial for future *in vivo* studies of silver NHC complexes having similar structures.

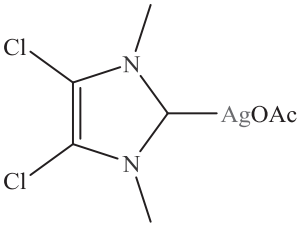

1

Conclusions

Based on the current and previous reports, benzimidazole-based bis-salts as well as respective dinuclear complexes are many fold more active than similar imidazole-based compounds. Ag(I)-NHC complexes were always relatively active when compared to the corresponding ligands. This provides evidence that silver cations play a vital role in the death of cancer cells. The photomicrographs of the cells treated with silver(I)-NHC complexes reveal clear signs of black silver in the cytoplasm of the affected cells, which confirms that the cytotoxic efficacy of the complexes is contributed by deposition of silver. Also, in dinuclear silver(I)-NHC complexes, cavity size and *N*-substitutions affect the anticancer potential of the compounds. Comparatively, larger cavity size is better for anticancer potential as well as longer alkyl chain length is better for cytotoxicity of Ag(I)-NHC complexes. The preliminary *in vivo* acute oral toxicity test results suggest non-toxic behavior in the biological system. *In vivo* anticancer studies are in progress and will be reported on completion.

Supplementary material

CCDC 924662 and CCDC 924661 contain the Supplementary crystallographic data for $\mathbf{L}_1$ and $\mathbf{C}_1$. This data can be obtained free of charge from http://www.ccdc.cam.ac.uk/conts/retrieving.html or from the Cambridge Crystallographic Data Center, 12 Union Road,

Cambridge CB2 1EZ, UK; Fax: 44-1223-336-033; or E-mail: deposit@ccdc.cam.ac.uk. Animals were obtained from ARASC USM Main campus under approval of Grant No. USM/Animals Ethics Approval/2012/(76) (364).

Acknowledgements

RAH thanks Universiti Sains Malaysia (USM) for the Research University (RU) Grant (1001/PKIMIA/811217) and short-term grant (1001/PKIMIA/823082). NH is grateful to (IPS) USM for the financial support [fellowship: RU(1001/441/CIPS/AUPE001)] and PRGS grant (1001/PKIMIA/834080). MAI is grateful to (IPS) USM for financial support [fellowship: USM.IPS/JWT/1/19 (JLD 6): P-KD0030/11(R)].

References

[1] F.E. Hahn, M.C. Jahnke. *Angew. Chem. Int. Ed.*, **47**, 3122 (2008).
[2] P.L. Arnold, S. Pearson. *Coord. Chem. Rev.*, **251**, 596 (2007).
[3] P.L. Arnold, I.J. Casely. *Chem. Rev.*, **109**, 3599 (2009).
[4] W.J. Evans. *Inorg. Chem.*, **46**, 3435 (2007).
[5] T. Weskamp, V.P.W. Böhm, W.A. Herrmann. *J. Organomet. Chem.*, **600**, 12 (2000).
[6] W.A. Herrmann. *Angew. Chem. Int. Ed.*, **41**, 1290 (2002).
[7] C.M. Crudden, D.P. Allen. *Coord. Chem. Rev.*, **248**, 2247 (2004).
[8] F. Glorius, S. Bellemin-Loponnaz, *Top. Organomet. Chem.*, **21**, 1 (2007).
[9] J.C. Garrison, W.J. Youngs. *Chem. Rev.*, **105**, 3978 (2005).
[10] M.L. Teyssot, A.S. Jarrousse, M. Manin, A. Chevry, S. Roche, F. Norre, C. Beaudoin, L. Morel, D. Boyer, R. Mahiou, A. Gautier. *Dalton Trans.*, 6894 (2009).
[11] I.J.B. Lin, C.S. Vasam. *Comments Inorg. Chem.*, **25**, 75 (2004).
[12] A.J. Arduengo, H.V.R. Dias, J.C. Calabrese, F. Davidson. *Organometallics*, **12**, 3405 (1993).
[13] J. Ramirez, R. Corberan, M. Sanau, E. Peris, E. Fernandez. *Chem. Commun. (Camb)*, 3056 (2005).
[14] A.C. Sentman, S. Csihony, R.M. Waymouth, J.L. Hedrick. *J. Org. Chem.*, **70**, 2391 (2005).
[15] A.C. Sentman, S. Csihony, G.W. Nyce, R.M. Waymouth, J.L. Hedrick. *Polym. Prepr.*, **45**, 299 (2004).
[16] W.A. Herrmann, M. Elison, J. Fischer, C. Köcher, G.R.J. Artus. *Angew. Chem. Int. Ed.*, **34**, 2371 (1995).
[17] B. Cornils, W.A. Herrmann (Eds.). *Aqueous-phase Organomet. Catal.: Concepts and Appl.*, Wiley-VCH, Weinheim, (2004).
[18] T.M. Trnka, R.H. Grubbs. *Acc. Chem. Res.*, **34**, 18 (2001).
[19] A.M. Caminade, V. Maraval, R. Laurent, J.P. Majoral. *Curr. Org. Chem.*, **6**, 739 (2002).
[20] K.M. Hindi, T.J. Siciliano, S. Durmus, M.J. Panzner, D.A. Medvetz, D.V. Reddy, L.A. Hogue, C.E. Hovis, J.K. Hilliard, R.J. Mallet, C.A. Tessier, C.L. Cannon, W.J. Youngs. *J. Med. Chem.*, **51**, 1577 (2008).
[21] S. Ray, R. Mohan, J.K. Singh, M.K. Samantaray, M.M. Shaikh, D. Panda, P. Ghosh. *J. Am. Chem. Soc.*, **129**, 15042 (2007).
[22] İ. Özdemir, E.Ö. Özcan, S. Günal, N. Gürbüz. *Molecules*, **15**, 2499 (2010).
[23] İ. Özdemir, S. Demir, S. Günal, İ. Özdemir, C. Arıcı, D. Ülkü. *Inorg. Chim. Acta*, **363**, 3803 (2010).
[24] B. Yığıt, Y. Gök, İ. Özdemır, S. Günal. *J. Coord. Chem.*, **65**, 371 (2012).
[25] A. Kascatan-Nebioglu, M.J. Panzner, C.A. Tessier, C.L. Cannon, W.J. Youngs. *Coord. Chem. Rev.*, **251**, 884 (2007).
[26] L. Eloy, A.S. Jarrousse, M.L. Teyssot, A. Gautier, L. Morel, C. Jolivalt, T. Cresteil, S. Roland. *ChemMedChem*, **7**, 805 (2012).
[27] C.H. Wang, W.C. Shih, H.C. Chang, Y.Y. Kuo, W.C. Hung, T.G. Ong, W.S. Li. *J. Med. Chem.*, **54**, 5245 (2011).
[28] G. Alves, L. Morel, M. El-Ghozzi, D. Avignant, B. Legeret, L. Nauton, F. Cisnetti, A. Gautier. *Chem. Commun.*, **47**, 7830 (2011).
[29] A. Gautier, F. Cisnetti. *Metallomics*, **4**, 23 (2012).
[30] W. Liu, R. Gust. *Chem. Soc. Rev.*, **42**, 755 (2013).
[31] L. Oehninger, R. Rubbiani, I. Ott. *Dalton Trans.*, 3269 (2013).
[32] S. Patil, A. Deally, B. Gleeson, H. Muller-Bunz, F. Paradisi, M. Tacke. *Metallomics*, **3**, 74 (2011).
[33] S. Patil, M. Tacke. *Monogr. Ser. Int. Conf. Coord. Bioinorg. Chem.*, **10**, 555 (2011).
[34] T.J. Siciliano, M.C. Deblock, K.M. Hindi, S. Durmus, M.J. Panzner, C.A. Tessier, W.J. Youngs. *J. Organomet. Chem.*, **696**, 1066 (2011).

[35] D.A. Medvetz, K.M. Hindi, M.J. Panzner, A.J. Ditto, Y.H. Yun, W.J. Youngs. *Met.-Based Drugs*, **2008**, 7 (year>2008). Article ID 384010, doi:10.1155/2008/384010.
[36] R. Haque, M. Iqbal, P. Asekunowo, A.M.S.A. Majid, M. Khadeer Ahamed, M. Umar, S. Al-Rawi, F. Al-Suede. *Med. Chem. Res.*, (2013). doi:10.1007/s00044-012-0461-8.
[37] R.A. Haque, S. Budagumpi, S.Y. Choo, M.K. Choong, B.E. Lokesh, K. Sudesh. *Appl. Organomet. Chem.*, **26**, 689 (2012).
[38] R.A. Haque, M.Z. Ghdhayeb, S. Budagumpi, A.W. Salman, M.B.K. Ahamed, A.M.S.A. Majid. *Inorg. Chim. Acta*, **394**, 519 (2013).
[39] R.A. Haque, M.A. Iqbal, P. Asekunowo, A.M.S.A. Majid, M.B. Khadeer Ahamed, M.I. Umar, S.S. Al-Rawi, F.S.R. Al-Suede. *Med. Chem. Res.*, (2013). doi:10.1007/s00044-012-0461-8.
[40] R.A. Haque, M.A. Iqbal, S. Budagumpi, M.B. Khadeer Ahamed, A.M.S. Abdul Majid, N. Hasanudin. *Appl. Organomet. Chem.*, **27**, 214 (2013).
[41] R.A. Haque, M.A. Iqbal, M.B. Khadeer, A.A. Majeed, Z.A. Abdul Hameed. *Chem. Cent. J.*, **6**, 68 (2012).
[42] M.A. Iqbal, R.A. Haque, S.F. Nasri, A.M.S. Abdul Majid, M.B. Khadeer Ahamed, E. Farsi, T. Fatima. *Chem. Cent. J.*, **7**, 27 (2013).
[43] M.A. Iqbal, R.A. Haque, M.B.K. Ahamed, M.A.M.S. Abdul, S. Al-Rawi. *Med. Chem. Res.*, **22**, 2455 (2013).
[44] M.A. Iqbal, R.A. Haque, S. Budagumpi, M.B. Khadeer Ahamed, A.M.S. Abdul Majid. *Inorg. Chem. Commun.*, **28**, 64 (2013).
[45] R.A. Haque, A.W. Salman, S. Budagumpi, A. Al-Ashraf Abdullah, A.M.S. Abdul Majid. *Metallomics*, **5**, 760 (2013).
[46] R.A. Haque, M.A. Iqbal, S. Budagumpi, M.B.K. Ahamed, A.M.A. Majid, N. Hasanudin. *Appl. Organomet. Chem.*, **27**, 214 (2013).
[47] R.A. Haque, S.F. Nasri, M.A. Iqbal. *J. Coord. Chem.*, **66**, 2679 (2013).
[48] D.M. Parkin, F. Bray, J. Ferlay, P. Pisani. *CA: A Cancer J. Clinicians*, **55**, 74 (2005).
[49] R. Haque, M. Iqbal, M. Khadeer, A. Majeed, Z. Abdul Hameed. *Chem. Cent. J.*, **6**, 68 (2012).
[50] M.V. Baker, D.H. Brown, R.A. Haque, B.W. Skelton, A.H. White. *Dalton Trans.*, 3756 (2004).
[51] M.A. Iqbal, R.A. Haque, S. Budagumpi, M.B.K. Ahamed, A.M.S.A. Majid. *Inorg. Chem. Commun.*, **28**, 64 (2013).
[52] R.A. Haque, M.Z. Ghdhayeb, A.W. Salman, S. Budagumpi, M.B. Khadeer Ahamed, A.M.S. Abdul Majid. *Inorg. Chem. Commun.*, **22**, 113 (2012).
[53] R.A. Haque, M.Z. Ghdhayeb, S. Budagumpi, A.W. Salman, M.B. Khadeer Ahamed, A.M.S.A. Majid. *Inorg. Chim. Acta*, **394**, 519 (2013).
[54] A.R. Knapp, M.J. Panzner, D.A. Medvetz, B.D. Wright, C.A. Tessier, W.J. Youngs. *Inorg. Chim. Acta*, **364**, 125 (2010).
[55] Q.-X. Liu, H.-L. Li, X.-J. Zhao, S.-S. Ge, M.-C. Shi, G. Shen, Y. Zang, X.-G. Wang. *Inorg. Chim. Acta*, **376**, 437 (2011).
[56] Q.-X. Liu, X.-J. Zhao, X.-M. Wu, L.-N. Yin, J.-H. Guo, X.-G. Wang, J.-C. Feng. *Inorg. Chim. Acta*, **361**, 2616 (2008).
[57] R.A. Haque, M.A. Iqbal, S.A. Ahmad, T.S. Chia, H.-K. Fun. *Acta Crystallogr., Sect. E*, **68**, o845 (2012).
[58] R.A. Haque, M.A. Iqbal, H.-K. Fun, S. Arshad. *Acta Crystallogr., Sect. E*, **68**, o924 (2012).
[59] R.A. Haque, M.A. Iqbal, M. Hemamalini, H.-K. Fun. *Acta Crystallogr., Sect. E*, **67**, o1814 (2011).
[60] R.A. Haque, S.F. Nasri, M. Hemamalini, H.-K. Fun. *Acta Crystallogr., Sect. E*, **67**, o1931 (2011).
[61] R.A. Haque, A.W. Salman, P. Nadarajan, M. Hemamalini, H.-K. Fun. *Acta Crystallogr., Sect. E*, **67**, o643 (2011).
[62] M.A. Iqbal, R.A. Haque, H.-K. Fun, T.S. Chia. *Acta Crystallogr. Sect. E*, **68**, o466 (2012).
[63] Q.-X. Liu, A.-H. Chen, X.-J. Zhao, Y. Zang, X.-M. Wu, X.-G. Wang, J.-H. Guo. *CrystEngComm*, **13**, 293 (2011).
[64] C.-Y. Liao, K.-T. Chan, P.-L. Chiu, C.-Y. Chen, H.M. Lee. *Inorg. Chim. Acta*, **361**, 2973 (2008).
[65] K.J. Soderlind, B. Gorodetsky, A. Singh, N. Bachur, G. Miller, J. Lown. *Anti-Cancer Drug Des.*, **14**, 19 (1999).
[66] A.T. Dinkova-Kostova, C. Abeygunawardana, P. Talalay. *J. Med. Chem.*, **41**, 5287 (1998).
[67] Y. Bansal, O. Silakari. *Bioorg. Med. Chem.*, **20**, 6208 (2012).
[68] B. Narasimhan, D. Sharma, P. Kumar. *Med. Chem. Res.*, **20**, 1119 (2011).
[69] B. Narasimhan, D. Sharma, P. Kumar. *Med. Chem. Res.*, **21**, 269 (2012).
[70] G. Gasser, N. Metzler-Nolte. *Curr. Opin. Chem. Biol.*, **16**, 84 (2012).
[71] D.C.F. Monteiro, R.M. Phillips, B.D. Crossley, J. Fielden, C.E. Willans. *Dalton Trans.*, 3720 (2012).
[72] H.Z. Zhang, S. Kasibhatla, J. Kuemmerle, W. Kemnitzer, K. Ollis-Mason, L. Qiu, C. Crogan-Grundy, B. Tseng, J. Drewe, S.X. Cai. *J. Med. Chem.*, **48**, 5215 (2005).
[73] W.J. Youngs, A.R. Knapp, P.O. Wagers, C.A. Tessier. *Dalton Trans.*, 327 (2012).
[74] D.-C. Zhong, Z.-F. Chen, Y.-C. Liu, X.-J. Luo, C. Barta, H. Liang. *J. Coord. Chem.*, **63**, 3146 (2010).
[75] A. Melaiye, W.J. Youngs. *Expert Opin. Ther. Patents*, **15**, 125 (2005).
[76] N. Meyer, E. Schuh, F. Mohr. *Annu. Rep. Prog. Chem. Sect. A: Inorg. Chem.*, **107**, 233 (2011).

[77] Y. Li, X. Dong, Y. Gou, Z. Jiang, H.-L. Zhu. *J. Coord. Chem.*, **64**, 1663 (2011).
[78] T.N.C. Wells, P. Scully, G. Paravicini, A.E.I. Proudfoot, M.A. Payton. *Biochemistry*, **34**, 7896 (1995).
[79] S.J. Tan, Y.K. Yan, P.P.F. Lee, K.H. Lim. *Future*, **2**, 1591 (2010).
[80] K. Nomiya, K. Tsuda, T. Sudoh, M. Oda. *J. Inorg. Biochem.*, **68**, 39 (1997).
[81] K. Nomiya, S. Takahashi, R. Noguchi, S. Nemoto, T. Takayama, M. Oda. *Inorg. Chem.*, **39**, 3301 (2000).
[82] K. Nomiya, H. Yokoyama. *J. Chem. Soc., Dalton Trans.*, 2483 (2002).
[83] C.G. Hartinger, P.J. Dyson. *Chem. Soc. Rev.*, **38**, 391 (2008).
[84] K.M. Hindi, M.J. Panzner, C.A. Tessier, C.L. Cannon, W.J. Youngs. *Chem. Rev.*, **109**, 3859 (2009).
[85] L. Mercs, M. Albrecht. *Chem. Soc. Rev.*, **39**, 1903 (2010).
[86] R. Snyder, C.C. Hedli. *Environ. Health Perspect.*, **104**, 1165 (1996).
[87] W.K. Lutz, C. Schlatter. *Chem. Biol. Interact.*, **18**, 241 (1979).
[88] R. Snyder, E. Lee, J. Kocsis. *Res. Commun. Chem. Pathol. Pharmacol.*, **20**, 191 (1978).
[89] T. Rushmore, R. Snyder, G. Kalf. *Chem Biol. Interact.*, **49**, 135 (1984).
[90] C. Graham. *Br. J. Nutr.*, **14**, S22 (2005).
[91] E. Walum. *Environ. Health Perspect.*, **106**, 497 (1998).
[92] E. Paget. *Acta Pharmacol. Toxicol.*, **52**, 6 (1983).
[93] OECD. Organisation for Economic Co-operation and Development. (2001). Link: http://iccvam.niehs.nih.gov/SuppDocs/FedDocs/OECD/OECD_GL420.pdf.
[94] P. Tamborini, H. Sigg, G. Zbinden. *Regul. Toxicol. Pharm.*, **12**, 69 (1990).